Metal ions control product specificity of isoprenyl diphosphate synthases in the insect terpenoid pathway

Sindy Frick[a], Raimund Nagel[b], Axel Schmidt[b], René R. Bodemann[a], Peter Rahfeld[a], Gerhard Pauls[a], Wolfgang Brandt[c], Jonathan Gershenzon[b], Wilhelm Boland[a], and Antje Burse[a,1]

Departments of [a]Bioorganic Chemistry and [b]Biochemistry, Max Planck Institute for Chemical Ecology, Beutenberg Campus, D-07745 Jena, Germany; and [c]Department of Bioorganic Chemistry, Leibniz Institute of Plant Biochemistry, D-06120 Halle/Saale, Germany

Edited by Jerrold Meinwald, Cornell University, Ithaca, NY, and approved January 29, 2013 (received for review December 12, 2012)

Isoprenyl diphosphate synthases (IDSs) produce the ubiquitous branched-chain diphosphates of different lengths that are precursors of all major classes of terpenes. Typically, individual short-chain IDSs (scIDSs) make the C_{10}, C_{15}, and C_{20} isoprenyl diphosphates separately. Here, we report that the product length synthesized by a single scIDS shifts depending on the divalent metal cofactor present. This previously undescribed mechanism of carbon chain-length determination was discovered for a scIDS from juvenile horseradish leaf beetles, *Phaedon cochleariae*. The recombinant enzyme *P. cochleariae* isoprenyl diphosphate synthase 1 (*Pc*IDS1) yields 96% C_{10}-geranyl diphosphate (GDP) and only 4% C_{15}-farnesyl diphosphate (FDP) in the presence of Co^{2+} or Mn^{2+} as a cofactor, whereas it yields only 18% C_{10} GDP but 82% C_{15} FDP in the presence of Mg^{2+}. In reaction with Co^{2+}, *Pc*IDS1 has a K_m of 11.6 μM for dimethylallyl diphosphate as a cosubstrate and 24.3 μM for GDP. However, with Mg^{2+}, *Pc*IDS1 has a K_m of 1.18 μM for GDP, suggesting that this substrate is favored by the enzyme under such conditions. RNAi targeting *Pc*IDS1 revealed the participation of this enzyme in the de novo synthesis of defensive monoterpenoids in the beetle larvae. As an FDP synthase, *Pc*IDS1 could be associated with the formation of sesquiterpenes, such as juvenile hormones. Detection of Co^{2+}, Mn^{2+}, or Mg^{2+} in the beetle larvae suggests flux control into C_{10} vs. C_{15} isoprenoids could be accomplished by these ions in vivo. The dependence of product chain length of scIDSs on metal cofactor identity introduces an additional regulation for these branch point enzymes of terpene metabolism.

cobalt | kinetic | prenyltransferase | secretions | silencing

Terpenes are an extensive group of natural products serving essential biological functions in Eukaryota, Bacteria, and Archaea. The more than 55,000 terpenes identified thus far are crucial components of intracellular signal-transduction pathways, electron transport chains, and membranes, or they can function as hormones, photosynthetic pigments, and semiochemicals (1, 2). Despite their structural diversity, terpenes are derived from the universal linear C_{10}, C_{15}, C_{20}, and larger diphosphate intermediates whose synthesis is catalyzed by isoprenyl diphosphate synthases (IDSs), also known as prenyltransferases (3). Depending on the stereochemistry of the double bond of the reaction product, these enzymes are classified as either *trans*-IDSs or *cis*-IDSs (4, 5).

Here, we focus on *trans*-IDSs, which can be further divided into enzymes producing short-chain (C_{10}–C_{20}), medium-chain (C_{25}–C_{35}), and long-chain (C_{40}–C_{50}) IDS products (6). Short-chain IDSs (scIDSs) are named for their main end products. Geranyl diphosphate synthases (GDPSs; EC 2.5.1.1) catalyze the alkylation of the homoallylic isopentenyl diphosphate (C_5-IDP) by the allylic dimethylallyl diphosphate (C_5-DMADP) resulting in geranyl diphosphate (GDP), the ubiquitous C_{10}-building block of many monoterpenes. Farnesyl diphosphate synthases (FDPSs; EC 2.5.1.10) form farnesyl diphosphate (FDP), the C_{15} precursor of sesquiterpenes, and geranylgeranyl diphosphate synthases (GGDPSs; EC 2.5.1.29) produce geranylgeranyl diphosphate (GGDP), the C_{20} backbone of diterpenes.

Whereas FDPSs and GGDPSs occur nearly ubiquitously in plants, animals, fungi, and bacteria, GDPSs have mainly been described in plants and insects to date (7). In plants, they participate in the biosynthesis of defenses against herbivores and pathogens, as well as in the formation of attractants for pollinators and seed-dispersing animals (1). Most plant GDPSs make GDP as a single product (8). However, occasionally, the enzymes are bifunctional and also produce FDP [*Pb*GDPS from the orchid *Phalaenopsis bellina* (9)] or GGDP [*Pa*IDS1 from the spruce *Picea abies* (10)] in addition to GDP. So far, only a few GDPSs have been characterized in insects (7). Strikingly, most of them have the ability to form multiple products.

The GDPSs cloned from the bark beetle *Ips pini*, for example, displayed prenyltransferase and terpene synthase activity in succession (11), resulting in the formation of precursors for the de novo synthesis of monoterpenoid aggregation pheromones such as ipsdienol, which coordinates the colonization of coniferous trees (12). Bifunctionality was also observed from the scIDSs characterized from different aphid species (13–17). Here, the recombinant proteins generated both GDP and FDP in parallel, and hence may be involved in the biosynthesis of either aphid sex pheromones or the sesquiterpene (*E*)-β-farnesene, the most common component of alarm pheromones. How nature accomplishes mixed-product formation by scIDSs in insects as well as in plants is still poorly understood.

Generally, catalysis by scIDSs follows a sequential mechanism called "head-to-tail alkylation." During chain elongation, the allylic cosubstrate (DMADP or GDP) undergoes coupling with IDP through electrophilic alkylation at its carbon-carbon double bond (18, 19). The reaction depends for activation on a trinuclear metal cluster, usually containing Mg^{2+} or Mn^{2+} (20). Based on earlier studies describing the role of metal cofactors for scIDS catalysis, we tested the product composition of a unique scIDS discovered from juvenile horseradish leaf beetles, *Phaedon cochleariae*, in the presence of different metal ions. To our surprise, we found that the enzyme *P. cochleariae* isoprenyl diphosphate synthase 1 (*Pc*IDS1) possesses an unusual product regulation mechanism not previously described for scIDSs. It alters the chain length of its products depending on the cofactor: The protein yields C_{10}-GDP in the presence of Co^{2+} or Mn^{2+}, whereas it produces the longer C_{15}-FDP in the presence of Mg^{2+}. GDP is needed for the de novo synthesis of the cyclopentanoid monoterpene iridoids, defensive compounds that are produced during the entire larval stage of *P. cochleariae* (21, 22) (Fig. 1). On the

Author contributions: S.F., A.S., J.G., W. Boland, and A.B. designed research; S.F., R.N., R.R.B., P.R., and G.P. performed research; J.G., W. Boland, and A.B. contributed new reagents/analytic tools; S.F., R.N., A.S., R.R.B., P.R., G.P., W. Brandt, and A.B. analyzed data; and S.F., A.S., J.G., W. Boland, and A.B. wrote the paper.

The authors declare no conflict of interest.

This article is a PNAS Direct Submission.

Data deposition: The *Pc*IDS1 sequence reported in this paper has been deposited in the GenBank database (accession no. KC109782) and the *Pc*IDS1 model has been deposited in the Protein Model DataBase (ID code PM0078683).

[1]To whom correspondence should be addressed. E-mail: aburse@ice.mpg.de.

This article contains supporting information online at www.pnas.org/lookup/suppl/doi:10.1073/pnas.1221489110/-/DCSupplemental.

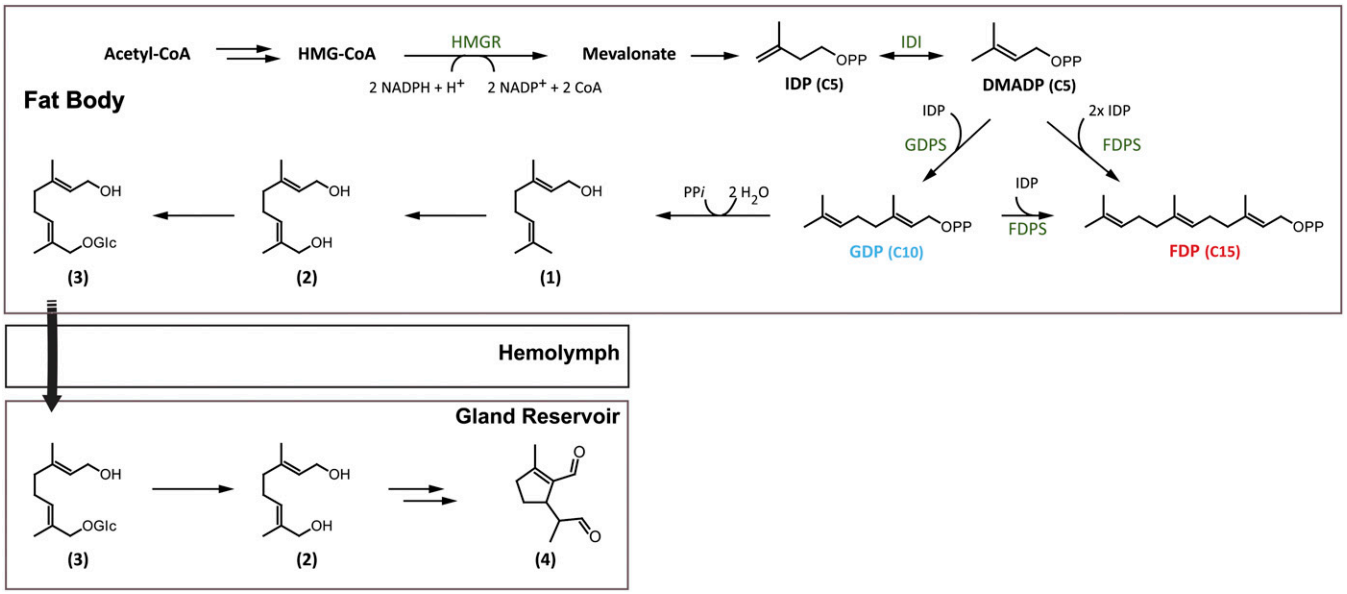

Fig. 1. Biosynthesis of iridoid monoterpene defenses in juvenile *P. cochleariae*: (1) geraniol, (2) 8-hydroxygeraniol, (3) 8-hydroxygeraniol-glucoside, (4) chrysomelidial. HMGR, 3-hydroxy-3-methyl-glutaryl-CoA reductase; IDI, isopentenyl diphosphate isomerase.

other hand, FDP serves as precursor for various primary metabolites and juvenile required hormone. The identification of Co^{2+}, Mn^{2+}, and Mg^{2+} in the juvenile beetles supports the notion that these organisms may control the product specificity of scIDSs by means of changes in local concentrations of these metal ions. Hence, the direction of flux at a branch point in terpene metabolism between defense and primary metabolism is regulated by an unprecedented IDS control mechanism.

Results

Identification and Tissue Distribution of a scIDS in Juvenile *P. cochleariae*. The use of degenerate primers allowed the amplification of a cDNA that encodes a protein of 430 aa (49.3 kDa, pI of 8.63) referred to here as *Pc*IDS1. ClustalW alignments revealed a high amino acid sequence identity of *Pc*IDS1 in relation to other functionally characterized insect scIDSs and showed all the conserved regions known for prenyltransferases (3, 23) (Fig. S1). The sequence also contains an RxxS motif (R_{67}–S_{70}), which could be the cleavage site for a mitochondrial targeting sequence already known from other identified scIDSs (11, 24).

Quantitative real-time assays revealed that *Pc*IDS1 transcripts are generally present in all analyzed larval tissues (Fig. S2*A*). However, the highest transcript abundance was observed in fat body tissue, which had a 5.6-fold higher transcript level compared with gut tissue. The transcript abundance was also reflected in protein level, because *Pc*IDS1 was detectable in all tested tissues, with the strongest signal derived from fat body tissue (Fig. S2*B*). Additionally, overall scIDS activity was determined in all crude extracts of the different larval tissues (Fig. 2*A*). In contrast to the trace amounts of FDP produced by extracts of every tissue tested, GDP-forming activity followed a different pattern. Compared with gut tissue, GDP formation was 141-fold higher in fat body tissue. Our results are consistent with recent findings on the distribution of the pathway to the iridoid defense compounds in *P. cochleariae* larvae. The early steps leading to the formation of the intermediate 8-hydroxygeraniol-glucoside are most likely localized in the fat body tissue. The glucoside is then transferred from there via the hemolymph into the defense glands, where the later steps in formation of chrysomelidial are located (25) (Fig. 1).

***Pc*IDS1 Is Involved in the Production of Defensive Monoterpenoids in Juvenile *P. cochleariae*.** RNAi experiments were performed with *P. cochleariae* to demonstrate the in vivo relevance of *Pc*IDS1. There were no significant differences in the relative growth rate between insects injected with a *PcIDS1*-dsRNA probe or with a control *Gfp* dsRNA probe and noninjected controls (NICs) (Fig. S3). However, transcript quantification 5 d after injection confirmed a significant *PcIDS1* mRNA reduction in fat body tissue (by 95%; $P < 0.001$) in comparison to *PcIDS1* mRNA levels in *Gfp*-treated larvae and NICs (Fig. 2*B*). Accordingly, 5 d after injection, the relative weight of defensive secretions decreased (by 52%; $P < 0.001$) in larvae challenged by *PcIDS1* dsRNA. This reduction continued until by day 13, a defenseless phenotype appeared that lacked secretions. The *Gfp* controls and NICs, on the other hand, produced unaltered amounts of defensive secretions (Fig. 2*C*). Detailed analyses of the relative amount of chrysomelidial per larva revealed a significant decline of this iridoid (by 78%; $P < 0.001$) in *PcIDS1*-treated larvae compared with the *Gfp* group and NICs after 5 d; this decline proceeded until there was a complete loss of secretions (Fig. 2*F*).

To determine if the chrysomelidial reduction is correlated with a decrease of the precursor, 8-hydroxygeraniol-glucoside, we analyzed the hemolymph and fat body tissue of larvae treated with *PcIDS1* dsRNA, *Gfp* dsRNA, and NICs. Seven days after *PcIDS1*-dsRNA injection, the level of precursor in the hemolymph was significantly reduced (by 89%; $P < 0.001$) compared with corresponding *Gfp* controls and NICs. This effect continued further with a reduction of 97% on day 11 (Fig. 2*E*). A similar effect was observed in the fat body tissue, where the amount of 8-hydroxygeraniol-glucoside was diminished (by 64.5 ± 14.08%) after 7 d. In addition to the reduction of chrysomelidial and 8-hydroxygeraniol-glucoside, we observed a significant loss of the overall scIDS activity (by 93%; $P < 0.001$) in the fat body tissue of *PcIDS1*-silenced larvae 7 d after injection compared with *Gfp* controls and NICs (Fig. 2*D*).

Recombinant *Pc*IDS1 Shows Metal Cofactor-Dependent Product Formation. Our results suggest that *Pc*IDS1 is involved in the biosynthesis of the monoterpenoid precursors needed for formation of the defensive compound chrysomelidial. Next, *Pc*IDS1 was expressed in *Escherichia coli* after truncation of the signal sequence at the 5′-end of the coding region, and the enzymatic activity of the purified recombinant protein was studied in vitro.

Like other scIDS proteins, *Pc*IDS1 was inactive without adding divalent metal cations, such as Mg^{2+} or Mn^{2+}. As recent

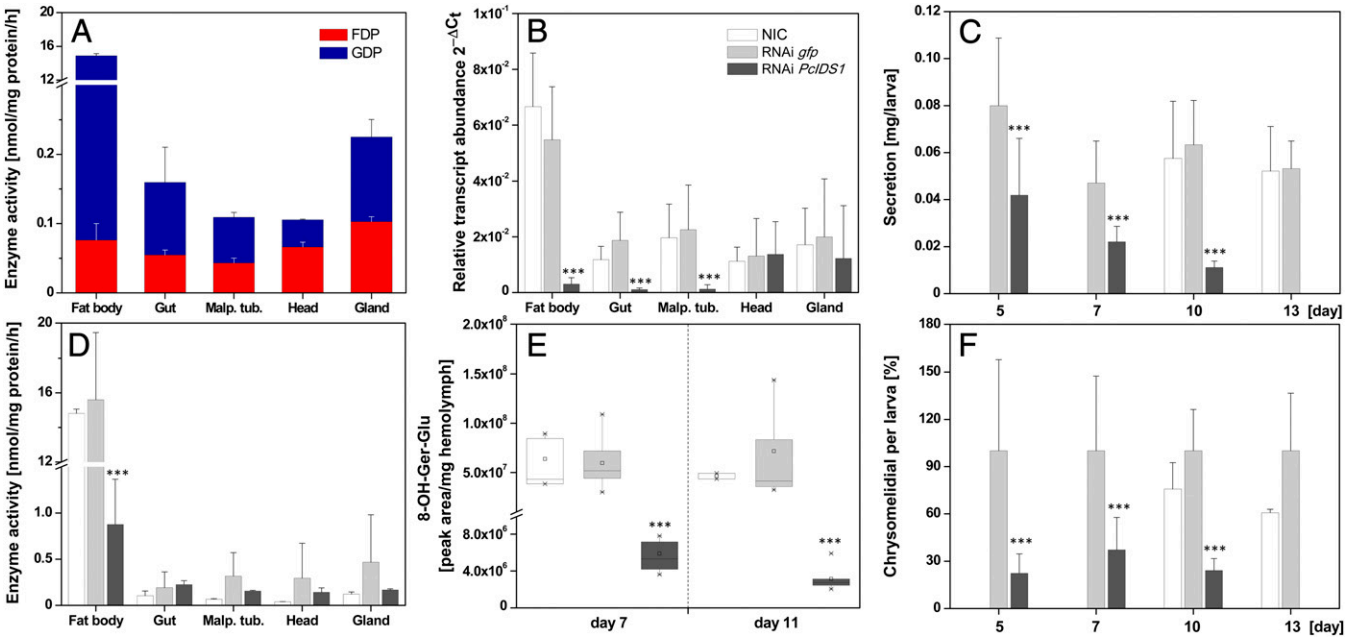

Fig. 2. Silencing *Pc*IDS1 in juvenile *P. cochleariae* by RNAi. (*A*) scIDS activity in tissue extracts of NICs: 10 μg of protein was incubated with 50 μM IDP, 50 μM DMADP, and 10 mM Mg^{2+} for 60 min ($n = 3$). (*B*) Relative transcript abundance ($2^{\Delta Ct}$) of *Pc*IDS1 in different larval tissues 5 d after dsRNA injection ($n = 3$, ±SD). (*C*) Relative weight of larval secretions observed at different time points after dsRNA injection ($n = 3$, ±SD). (*D*) scIDS activity in tissues extracts 7 d after dsRNA injection. Ten micrograms of protein was incubated with 50 μM IDP, 50 μM DMADP, and 10 mM Mg^{2+} for 60 min ($n = 3$, ±SD). (*E*) Amount of 8-hydroxygeraniol-glucoside (8-OH-Ger-Glu) in hemolymph by HPLC analyses after dsRNA injection ($n = 3$, ±SD). (*F*) GC-MS analyses of chrysomelidial after dsRNA injection ($n = 3$, ±SD). Malp. tub., Malpighian tubules. ***, $p < 0.001$.

studies show, scIDS activity can be modulated by these metal ion cofactors (7, 15, 16, 26, 27); we therefore tested *Pc*IDS1 activity with IDP and two different allylic substrates, DMADP and GDP, in the presence of five different divalent cations. Each ion was tested separately at comparable concentration ranges.

In our assays with DMADP, the maximum overall enzyme activity for each cation was observed at 5 mM for Mg^{2+}, 0.5 mM for Co^{2+} and Mn^{2+}, and 0.1 mM for Ni^{2+} and Zn^{2+} (Fig. 3*A*, Fig. S4*A*, and Table S1). *Pc*IDS1 was far more active with Co^{2+} as an additive than with any other tested metal ion. Intriguingly, not only the overall enzyme activity but the product specificity varied considerably according to the different ions. In the presence of Co^{2+} or Mn^{2+}, with DMADP as a cosubstrate, *Pc*IDS1 produced about 96% GDP and only 4% FDP. In contrast, with Mg^{2+} as an additive, *Pc*IDS1 produced 18% GDP and 82% FDP.

Moreover, the optimal ion concentration changed depending on the allylic substrates. After GDP was substituted for DMADP, leading to the production of FDP, we observed *Pc*IDS1 being most active by addition of 0.5 mM Mg^{2+} compared with any other tested cofactor (Fig. 3*B*, Fig. S4*B*, and Table S1). Overall, Mg^{2+}, Mn^{2+}, and Co^{2+} represent the cofactors most favored in *Pc*IDS1 catalysis. Because Co^{2+} and Mg^{2+} resulted in the highest levels of *Pc*IDS1 activity, we used these cofactors in the following experiments.

In a first approach with DMADP, a constant Co^{2+} concentration of 0.5 mM was complemented with an ascending concentration of Mg^{2+} in a range of 0.001–10 mM (Fig. 4*A*). *Pc*IDS1 formed mainly GDP and only minor amounts of FDP, suggesting that Co^{2+} is the dominant metal ion independent of the tested Mg^{2+} concentration.

In a second approach with DMADP, we measured the enzyme activity with Mg^{2+} constant at 5 mM and an ascending concentration of Co^{2+} in the range of 0.001–10 mM (Fig. 4*B*). At Co^{2+} concentrations lower than 0.05 mM, FDP was the main product, accompanied by a 50% reduction in enzyme activity. However, if Co^{2+} concentrations exceeded 0.1 mM, *Pc*IDS1 activity clearly increased. Simultaneously, a shift from FDP to the reduced chain length of GDP was observed. Even if Mg^{2+} was 100-fold more abundant in the mixture, the enzyme definitely showed a preference for Co^{2+}.

With GDP as a cosubstrate, a constant 0.5 mM Co^{2+}, and an ascending Mg^{2+} concentration, *Pc*IDS1 displayed low FDP-forming activity (Fig. 4*C*). If Mg^{2+} is constant at 5 mM and Co^{2+} concentrations vary, we observed high FDP production only at Co^{2+} concentrations below 0.1 mM. However, as soon as the Co^{2+} concentration ascends, the FDP-forming activity decreases dramatically (Fig. 4*D*). Our findings indicate that the Mg^{2+}-catalyzed activity of *Pc*IDS1 is abolished as soon as Co^{2+} reaches its optimal concentration.

To determine the conformational state of *Pc*IDS1 quaternary structure, size exclusion chromatography was performed. Fig. S5 shows the relative retention volumes of the apoprotein without adding cofactors and *Pc*IDS1 in presence of Co^{2+} (0.5 mM) or Mg^{2+} (5 mM). Surprisingly, we found an obvious difference in the elution volume among the apoprotein (without divalent metal), the *Pc*IDS1-Mg^{2+} complex, and the *Pc*IDS1-Co^{2+} complex. The apoprotein eluted from the column at a retention volume of 76.36 mL (corresponding to 74.6 kDa), whereas *Pc*IDs1-Mg^{2+} and *Pc*IDS1-Co^{2+} eluted at 73.65 mL (corresponding to 93.8 kDa) and 74.46 mL (corresponding to 87.6 kDa), respectively. Given the calculated monomeric mass of 45.8 kDa, this indicates on one hand that the enzyme is always present as a dimer regardless of added cofactor. On the other hand, the difference in the elution volume reflects a change in the hydrodynamic volume of the protein caused by the divalent metal. In the case of Mg^{2+}, the dimeric protein possesses the largest volume, most likely due to a more relaxed conformation. With Co^{2+}, *Pc*IDS1 seems to have a more compact conformation, which may be responsible for the change in product spectrum. As a control, we also analyzed the metal influence on the standard proteins and observed no obvious difference in the elution volume with addition of various amounts of Mg^{2+} or Co^{2+}.

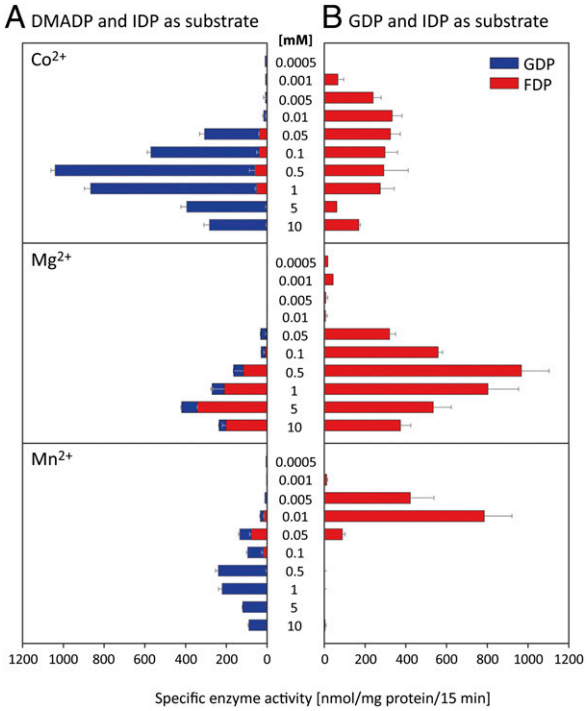

Fig. 3. Effect of metal cofactors on enzyme activity and product formation of *Pc*IDS1. (*A*) Different concentrations of Co^{2+}, Mg^{2+}, and Mn^{2+} were added to *Pc*IDS1 and incubated with 50 μM IDP and 50 μM DMADP ($n = 3$, ±SD). (*B*) Different concentrations of Co^{2+}, Mg^{2+}, and Mn^{2+} were added to *Pc*IDS1 and incubated with 50 μM IDP and 50 μM GDP ($n = 3$, ±SD).

Kinetic Analyses of Purified *Pc*IDS1. All kinetic parameters measured for *Pc*IDS1 are displayed in Table 1. In combination with Co^{2+} and fixed IDP, *Pc*IDS1 has a K_m of 11.6 μM for DMADP (Fig. S6*A*) and a K_m of 24.3 μM for GDP (Fig. S6*E*), suggesting that DMADP is the preferred substrate compared with GDP. Significant differences in the V_{max} were not observed. With Co^{2+} and DMADP fixed at 50 μM, *Pc*IDS1 has a K_m of 0.8 μM for IDP and substrate inhibition at higher concentrations with a K_i of 46.6 μM (Fig. S6*B*). No inhibitory effect of IDP was observed with GDP fixed at 50 μM (Fig. S6*F*).

In combination with Mg^{2+} and fixed IDP, *Pc*IDS1 displayed atypical kinetics for DMADP that resulted in a biphasic curve (Fig. S6*C*). In the first part of the curve from 0.1 to 100 μM DMADP, the reaction seems to follow a Michaelis–Menten kinetic. However, the curve displays a different slope as soon as the DMADP concentration exceeds 50 μM. The K_m for GDP was 1.2 μM with a slight substrate inhibition (Fig. S6*G*). With Mg^{2+} and DMADP fixed at 50 μM, *Pc*IDS1 has a K_m of 11.8 μM for IDP with a slight substrate inhibition (Fig. S6*D*), and with GDP fixed at 50 μM, the K_m of IDP was 7.1 μM (Fig. S6*H*). Analyses of the calculated V_{max} show that Mn^{2+} gave generally lower reaction velocities than did Co^{2+}.

The kinetic parameters substantiate our previous observations that *Pc*IDS1 has a preference for Co^{2+} with DMADP as an allylic cosubstrate giving the C_{10} product GDP. If Mg^{2+} is the metal cofactor, GDP is the favored cosubstrate affording the C_{15} product FDP.

Metal Cofactors Identified in *P. cochleariae* Larvae Have Different Affinities in the Enzyme Complex. Inductively coupled plasma-MS analysis of *P. cochleariae* larvae showed an overall concentration of Co^{2+} in the fat body tissue at ≥0.24 μg/g of dry weight (DW) or 4 nmol/g of DW, and an overall concentration of Mn^{2+} at ≥16.6 μg/g of DW or 0.3 μmol/g of DW, whereas Mg^{2+} was found at a concentration of 2,223 μg/g of DW or 91 μmol/g of DW in the fat body (Table S2).

Quantum mechanical calculations revealed reaction energies of about 40 kcal/mol lower for the formation of complexes containing Co^{2+} or Mn^{2+} compared with those containing Mg^{2+} for association with the diphosphate of DP^{3-} or the aspartate residues of the enzyme (mimicked by propionic acid anions) (Tables S3 and S4). In all cases, the affinity of the metal cations for the diphosphate was more than 200 kcal/mol higher than for the aspartate residues. Based on these gas phase calculations, the deduced minimum equilibrium constant for formation of the diphosphate metal complex is at least 10^{28}-fold higher for Co^{2+} or Mn^{2+} than for Mg^{2+}, which suggests that *Pc*IDS1 may have a considerably higher affinity for Co^{2+} or Mn^{2+} than for Mg^{2+}, although the magnitude of this difference may be reduced somewhat by solvation effects not considered here. Hence, the low concentrations of Co^{2+} or Mn^{2+} in the larval tissue in comparison to Mg^{2+} may be compensated for by their greater complex formation ability with diphosphate. On the other hand, if one compares the affinities of either the metal ion-complexed diphosphate with the aspartate (assuming the metal cations are delivered to the binding site together with the substrate) or, alternatively, the metal-complexed aspartates with the diphosphate (Tables S5 and S6), in both cases, the affinities for Co^{2+} or Mn^{2+} are lower than the affinity for Mg^{2+} in nice agreement with the measured lower $K_{m\,(GDP)}$ (higher affinity) ($Mg^{2+} = 1.18$ μM, $Co^{2+} = 24.3$ μM) and might be an explanation for the experimental differences in product specificity with different divalent metal ions. Note, one order of magnitude in K_m represents 1.4 kcal/mol (ΔG) in interaction energies.

Discussion

Understanding the mechanism of chain-length determination of scIDSs has been a major challenge for researchers of terpene biosynthetic enzymes, and much has been learned about active site features that restrict the length of the enzyme products. The determination of product carbon length by the identity of the metal cofactor apparently provides an alternative mechanism to the regulation of product formation by scIDS. Given that plants possess a number of genes encoding IDSs [e.g., at least 10 in *Arabidopsis thaliana* (8)], whereas insects possess only a few [e.g., 3 in *Bombyx mori* (28)], insects may compensate for this disparity by generating different chain-length products in other ways. In our case, the metal ion-mediated product differences enable the *P. cochleariae* beetles to supply precursors for two terpene pathways, one for monoterpene metabolism (synthesis of chemical defenses) and one for sesquiterpene metabolism (juvenile hormone formation), using only a single enzyme. Instead of "inventing" a new IDS, insects appear to use different cofactors to add an additional product to an enzyme's repertoire, thereby lowering metabolic costs. Such a regulation mechanism may allow faster adaptation to developmental or environmental changes that insects may face, such as metamorphosis or host plant shifts. Due to differences in metal ion identity and concentration, shifts in overall scIDS activity have previously been observed for enzymes from plants [e.g., *Abies grandis* (29)] and for enzymes from insects [e.g., *Myzus persicae* (15), *Choristoneura fumiferana* (30)], but without alterations in product chain length. However, Sen et al. (26) report cofactor-dependent changes of product chain length in crude homogenates of the *corpora allata* of the lepidopteran *Manduca sexta*. The product ratios formed during the coupling of DMADP with IDP by means of scIDS activity showed that FDP formation was stimulated by adding Mg^{2+}, whereas GDP formation increased in the presence of Mn^{2+}. Taken together with our results, these findings should motivate researchers to test alternative cofactors with scIDSs in the future.

*Pc*IDS1 produces mainly GDP (95%) in the presence of Co^{2+} (or Mn^{2+}) with IDP and DMADP as substrates and produces only minor amounts of FDP (4%). In contrast, with Mg^{2+}, the predominant product was FDP (82%); only minor amounts of GDP (18%) were produced. Our kinetic data for *Pc*IDS1 support the observation that the regulation of product distribution by these metal cofactors is biochemically relevant. Comparisons

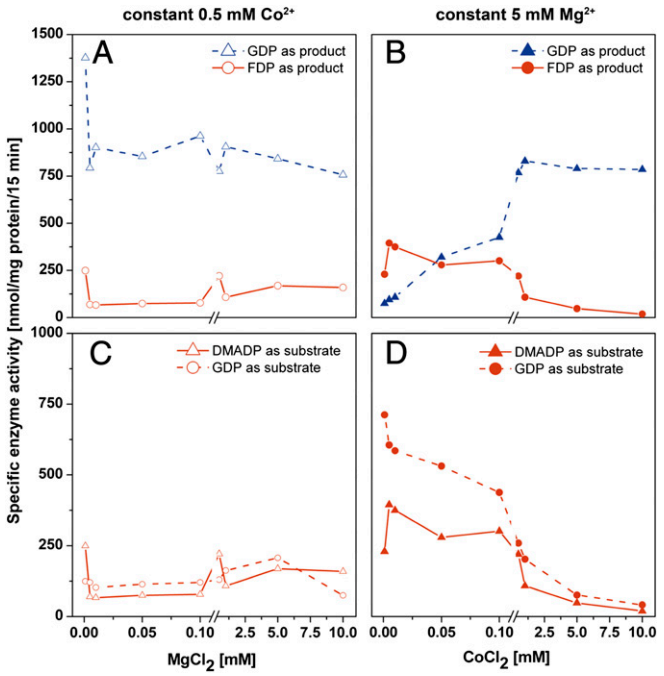

Fig. 4. Effect of mixtures of divalent metal ion cofactors on enzyme activity and product formation of *Pc*IDS1. (*A*) Constant 0.5 mM Co^{2+} with an ascending Mg^{2+} concentration in a range of 0.001 mM up to 10 mM with 50 μM IDP or 50 μM DMADP ($n = 2$). (*B*) Constant 5 mM Mg^{2+} with an ascending Co^{2+} concentration from 0.001 mM up to 10 mM with 50 μM IDP or 50 μM DMADP ($n = 2$). (*C*) FDP formation at constant 0.5 mM Co^{2+} with an ascending Mg^{2+} concentration with 50 μM GDP or 50 μM DMADP ($n = 2$). (*D*) FDP formation at constant 5 mM Mg^{2+} with an ascending Co^{2+} concentration with 50 μM GDP or 50 μM DMADP ($n = 2$).

with kinetic data available from plant GDPSs in the presence of DMADP revealed that the $K_{m(DMADP)}$ of *Pc*IDS1 (11.6 μM) with Co^{2+} corresponds to the K_m of the enzyme from *Anthirrhium majus* (24.1 μM) (31) or *Anthirrhium grandis* (16.7 μM) (29). $K_{m(DMADP)}$ values from insect scIDSs have so far been determined only for the bifunctional GDPSs of *M. persicae* *Mp*IPPS1-S (28.6 μM) (17) and *Mp*IPPS2-S (24.2 μM) (17), as well as *Aphis gossypii* (39.2 μM) (14), and for the FDPS from *Drosophila melanogaster* *Dm*FPPS-1b (33.5 μM) (32). The K_m of *Pc*IDS1 is found within the range of literature values. The combination of DMADP with Mg^{2+} did not allow a K_m calculation due to the biphasic progression of the kinetic curve. Although DMADP reacts initially with IDP to form GDP, in later catalytic cycles, the GDP formed can compete with another molecule of DMADP at the allylic binding site of *Pc*IDS1. If GDP is the preferred allylic substrate in combination with Mg^{2+}, it can lead to the formation of FDP.

The K_m values of *Pc*IDS1 for GDP, which are 24.3 μM and 1.1 μM in the presence of Co^{2+} and Mg^{2+}, respectively, are in the range of K_m values for previously described insect scIDSs, such as those of *A. gossypii* (12.6 μM) (14), *D. melanogaster* FPPS-1b (7 μM) (32), *M. sexta* (0.8 μM) (27), and *M. persicae* (*Mp*IPPS1-S, 25.4 μM; *Mp*IPPS2-S, 15.4 μM) (17). The difference in the *Pc*IDS1 K_m values for different metal cofactors suggests that the enzyme favors GDP as a substrate with Mg^{2+}. The alteration of IDS product specificity by metal ions has so far been described only for long-chain IDSs from microbes. In the presence of Co^{2+} or Mn^{2+}, octaprenyl-, solanesyl-, and decaprenyl-diphosphate synthases gave a variety of polyprenyl products whose chains were longer by up to two isoprene units than those of the products formed in the presence of Mg^{2+} (33–35).

IDS structure elucidation in combination with mutagenesis studies has suggested that product chain length is determined by the size of the hydrophobic pocket in the active center. In particular, the amino acids in the vicinity of the conserved first and second aspartate-rich regions (FARM and SARM motifs, respectively) form a steric hindrance that terminates chain elongation (3, 23, 36, 37). The van der Waals radii of Co^{2+} and Mn^{2+} are 1.73 Å and 1.9 Å, respectively, both of which are larger than that of Mg^{2+} at 0.96 Å (38). These differences may lead to conformational changes of *Pc*IDS1 or to rearrangements of substrate position in the enzymes that influence chain-length elongation. First hints toward conformational changes were obtained by size exclusion chromatography that revealed differences in the quaternary structure due to complex formation with different metal ions. Further homology modeling in combination with site-directed amino acid mutagenesis is needed to explain more fully how changes in cofactors influence the chain-length determination mechanism for *Pc*IDS1.

Mg^{2+} and Mn^{2+} are well-known cofactors for scIDS activity; however, in our biochemical characterization, *Pc*IDS1 showed the highest GDP synthase activity in the presence of Co^{2+}. Despite its rare occurrence in nature, Co^{2+} plays a role as a cofactor in a number of proteins (e.g., methionine aminopeptidase, glucose isomerase) (39). To balance the need for cobalt with its intrinsic toxicity, nature has evolved trafficking systems to maintain metal homeostasis (40). For example, in the transcriptome from *P. cochleariae*, we have identified a transport protein that shows high similarity to the cobalt uptake protein Cot 1 of *Saccharomyces cerevisiae* (41). This finding and the calculated high affinity of Co^{2+} to *Pc*IDS1 underline the possibility that Co^{2+} is an available as well as biologically relevant cofactor for this enzyme despite its low concentration in the larvae.

Using an RNAi approach, we were able to show that the *Pc*IDS1-catalyzed formation of GDP is involved in the production of monoterpenoid defensive compounds in *P. cochleariae* larvae. However, we could not detect a phenotype arising from the loss of formation of the alternate product, FDP. In insects, FDP is the essential precursor for the synthesis of juvenile hormones (42), and it is localized in the *corpora allata* complex found in the head posterior to the brain. Given that RNAi efficiency can differ from tissue to tissue as well as from gene to gene (43), the lack of a phenotype caused by low FDP levels might be attributed to ineffective silencing in the larval head. However, even more important may be the existence of additional prenyltransferases. Aphids, coleopterans, and lepidopterans are known to possess up to three scIDSs, and we are currently searching for additional scIDSs in *P. cochleariae*, which, like many other

Table 1. Kinetic constants for *P. cochleariae* *Pc*IDS1 depend on the identity of both the metal cofactor and allylic substrate

	Co^{2+}				Mg^{2+}			
Fixed substrate	$IDP_{(15\ \mu M)}$	$IDP_{(50\ \mu M)}$	$DMADP_{(50\ \mu M)}$	$GDP_{(50\ \mu M)}$	$IDP_{(50\ \mu M)}$	$IDP_{(50\ \mu M)}$	$DMADP_{(50\ \mu M)}$	$GDP_{(50\ \mu M)}$
Substrate	DMADP	GDP	IDP	IDP	DMADP	GDP	IDP	IDP
$K_{m\ (substrate)}$, μM	11.60	24.31	0.84	1.46	~1103	1.19	11.79	7.08
V_{max}, μmol·min^{-1}·mg^{-1} of protein	0.44	0.41	0.67	0.23	~2.39	0.12	0.17	0.20
$K_{i\ (substrate)}$, μM	n.d.	n.d.	46.62	n.d.	n.d.	1,047	572.7	322.1

n.d., not detectable.

enzymes of this class, may make more than one product. Our work shows that enzymes with an intrinsic promiscuity may also use exogenous factors, such as metal cofactors, to regulate product synthesis. It also serves as a reminder that neither substrate specificity nor product profiles can always be predicted by sequence similarity. Instead, rigorous biochemical testing is needed to establish enzyme function, especially among enzymes of terpene metabolism.

Materials and Methods

A scIDS from *P. cochleariae* was isolated with a degenerated PCR approach and RACE amplification. For further biochemical characterization, heterologous expression in *E. coli* Bl21 star (DE3) and protein purification were performed by affinity chromatography with Ni-nitrilotriacetric acid agarose columns. RNAi techniques were used to determine in vivo relevance, followed by quantitative real-time PCR, the quantification of 8-hydroxygeraniol via liquid chromatography (LC)-tandem MS (MS/MS), the relative quantification of chrysomelidial with GC-MS, and *Pc*IDS1 activity measurements determined by LC-MS/MS. Kinetic analyses and product determination were realized by LC-MS/MS, and calculations were performed with GraphPad Prism (GraphPad Software). Details of beetle rearing, reagents, protein purification/sequencing, antibody production, RNAi techniques, LC-MS/MS, GC-MS, quantitative PCR, sequence analyses, and other methods used in this study are described in *SI Materials and Methods*.

ACKNOWLEDGMENTS. We thank Dr. Dirk Merten for the element analysis and Angelika Berg and Dr. Maritta Kunert for technical assistance. We thank Prof. Jacques M. Pasteels for helpful discussions on aspects of this work and Emily Wheeler for critically reading of the manuscript. This work has been supported by the Deutsche Forschungsgemeinschaft (Grant BU 1862/2-1) and the Max Planck Society.

1. Gershenzon J, Dudareva N (2007) The function of terpene natural products in the natural world. *Nat Chem Biol* 3(7):408–414.
2. Pichersky E, Noel JP, Dudareva N (2006) Biosynthesis of plant volatiles: Nature's diversity and ingenuity. *Science* 311(5762):808–811.
3. Wang KC, Ohnuma S (2000) Isoprenyl diphosphate synthases. *Biochim Biophys Acta* 1529(1-3):33–48.
4. Kharel Y, Koyama T (2003) Molecular analysis of cis-prenyl chain elongating enzymes. *Nat Prod Rep* 20(1):111–118.
5. Liang PH (2009) Reaction kinetics, catalytic mechanisms, conformational changes, and inhibitor design for prenyltransferases. *Biochemistry* 48(28):6562–6570.
6. Gershenzon J, Kreis J (1999) Biochemistry of terpenoids: Monoterpenes, sesquiterpenes, diterpenes, sterols, cardiac glycosides, and steroid saponins. *Biochemistry of Plant Secondary Metabolism*, ed Wink M (Sheffield Academic, Sheffield, UK), pp 222–299.
7. Vandermoten S, Haubruge E, Cusson M (2009) New insights into short-chain prenyltransferases: Structural features, evolutionary history and potential for selective inhibition. *Cell Mol Life Sci* 66(23):3685–3695.
8. Tholl D, Lee S (2011) Terpene specialized metabolism in *Arabidopsis thaliana*. *The Arabidopsis Book*, ed Last R (American Society of Plant Biologists, Rockville, MD), Vol 9, pp e0143.
9. Hsiao YY, et al. (2008) A novel homodimeric geranyl diphosphate synthase from the orchid Phalaenopsis bellina lacking a DD(X)2-4D motif. *Plant J* 55(5):719–733.
10. Schmidt A, et al. (2010) A bifunctional geranyl and geranylgeranyl diphosphate synthase is involved in terpene oleoresin formation in *Picea abies*. *Plant Physiol* 152(2):639–655.
11. Gilg AB, Bearfield JC, Tittiger C, Welch WH, Blomquist GJ (2005) Isolation and functional expression of an animal geranyl diphosphate synthase and its role in bark beetle pheromone biosynthesis. *Proc Natl Acad Sci USA* 102(28):9760–9765.
12. Blomquist GJ, et al. (2010) Pheromone production in bark beetles. *Insect Biochem Mol Biol* 40(10):699–712.
13. Lewis MJ, Prosser IM, Mohib A, Field LM (2008) Cloning and characterisation of a prenyltransferase from the aphid *Myzus persicae* with potential involvement in alarm pheromone biosynthesis. *Insect Mol Biol* 17(4):437–443.
14. Ma G-Y, Sun XF, Zhang YL, Li ZX, Shen ZR (2010) Molecular cloning and characterization of a prenyltransferase from the cotton aphid, *Aphis gossypii*. *Insect Biochem Mol Biol* 40(7):552–561.
15. Vandermoten S, et al. (2008) Characterization of a novel aphid prenyltransferase displaying dual geranyl/farnesyl diphosphate synthase activity. *FEBS Lett* 582(13): 1928–1934.
16. Vandermoten S, et al. (2009) Structural features conferring dual geranyl/farnesyl diphosphate synthase activity to an aphid prenyltransferase. *Insect Biochem Mol Biol* 39(10):707–716.
17. Zhang Y-L, Li Z-X (2012) Functional analysis and molecular docking identify two active short-chain prenyltransferases in the green peach aphid, *Myzus persicae*. *Arch Insect Biochem Physiol* 81(2):63–76.
18. Oldfield E, Lin FY (2012) Terpene biosynthesis: Modularity rules. *Angew Chem Int Ed Engl* 51(5):1124–1137.
19. Brandt W, et al. (2009) Molecular and structural basis of metabolic diversity mediated by prenyldiphosphate converting enzymes. *Phytochemistry* 70(15-16):1758–1775.
20. Aaron JA, Christianson DW (2010) Trinuclear metal clusters in catalysis by terpenoid synthases. *Pure Appl Chem* 82(8):1585–1597.
21. Pasteels JM, Braekman JC, Daloze D, Ottinger R (1982) Chemical defence in chrysomelid larvae and adults. *Tetrahedron* 38(13):1891–1897.
22. Termonia A, Hsiao TH, Pasteels JM, Milinkovitch MC (2001) Feeding specialization and host-derived chemical defense in Chrysomeline leaf beetles did not lead to an evolutionary dead end. *Proc Natl Acad Sci USA* 98(7):3909–3914.
23. Tarshis LC, Proteau PJ, Kellogg BA, Sacchettini JC, Poulter CD (1996) Regulation of product chain length by isoprenyl diphosphate synthases. *Proc Natl Acad Sci USA* 93(26):15018–15023.
24. von Heijne G (1990) The signal peptide. *J Membr Biol* 115(3):195–201.
25. Burse A, et al. (2008) Implication of HMGR in homeostasis of sequestered and *de novo* produced precursors of the iridoid biosynthesis in leaf beetle larvae. *Insect Biochem Mol Biol* 38(1):76–88.
26. Sen SE, Brown DC, Sperry AE, Hitchcock JR (2007) Prenyltransferase of larval and adult M. sexta corpora allata. *Insect Biochem Mol Biol* 37(1):29–40.
27. Sen SE, Sperry AE (2002) Partial purification of a farnesyl diphosphate synthase from whole-body Manduca sexta. *Insect Biochem Mol Biol* 32(8):889–899.
28. Kaneko Y, Kinjoh T, Kiuchi M, Hiruma K (2011) Stage-specific regulation of juvenile hormone biosynthesis by ecdysteroid in *Bombyx mori*. *Mol Cell Endocrinol* 335(2): 204–210.
29. Tholl D, Croteau R, Gershenzon J (2001) Partial purification and characterization of the short-chain prenyltransferases, geranyl diphosphate synthase and farnesyl diphosphate synthase, from Abies grandis (grand fir). *Arch Biochem Biophys* 386(2):233–242.
30. Sen SE, et al. (2007) Purification, properties and heteromeric association of type-1 and type-2 lepidopteran farnesyl diphosphate synthases. *Insect Biochem Mol Biol* 37(8): 819–828.
31. Tholl D, et al. (2004) Formation of monoterpenes in *Antirrhinum majus* and *Clarkia breweri* flowers involves heterodimeric geranyl diphosphate synthases. *Plant Cell* 16(4):977–992.
32. Sen SE, Trobaugh C, Béliveau C, Richard T, Cusson M (2007) Cloning, expression and characterization of a dipteran farnesyl diphosphate synthase. *Insect Biochem Mol Biol* 37(11):1198–1206.
33. Ohnuma S, Koyama T, Ogura K (1992) Chain length distribution of the products formed in solanesyl diphosphate synthase reaction. *J Biochem* 112(6):743–749.
34. Ohnuma S, Koyama T, Ogura K (1993) Alteration of the product specificities of prenyltransferases by metal ions. *Biochem Biophys Res Commun* 192(2):407–412.
35. Fujii H, et al. (1980) Variable product specificity of solanesyl pyrophosphate synthetase. *Biochem Biophys Res Commun* 96(4):1648–1653.
36. Chen AJ, Kroon PA, Poulter CD (1994) Isoprenyl diphosphate synthases: Protein sequence comparisons, a phylogenetic tree, and predictions of secondary structure. *Protein Sci* 3(4):600–607.
37. Szkopińska A, Płochocka D (2005) Farnesyl diphosphate synthase; regulation of product specificity. *Acta Biochim Pol* 52(1):45–55.
38. Heuts JPA, Schipper E, Piet P, German AL (1995) Molecular mechanics calculations on cobalt phthalocyanine dimers. *Theochem-J Mol Struct* 333(1-2):39–47.
39. Kobayashi M, Shimizu S (1999) Cobalt proteins. *Eur J Biochem* 261(1):1–9.
40. Okamoto S, Eltis LD (2011) The biological occurrence and trafficking of cobalt. *Metallomics* 3(10):963–970.
41. Conklin DS, McMaster JA, Culbertson MR, Kung C (1992) COT1, a gene involved in cobalt accumulation in Saccharomyces cerevisiae. *Mol Cell Biol* 12(9):3678–3688.
42. Bellés X, Martín D, Piulachs MD (2005) The mevalonate pathway and the synthesis of juvenile hormone in insects. *Annu Rev Entomol* 50:181–199.
43. Terenius O, et al. (2011) RNA interference in Lepidoptera: An overview of successful and unsuccessful studies and implications for experimental design. *J Insect Physiol* 57(2):231–245.